Beamlike twin-photon generation by use of type II parametric downconversion

Shigeki Takeuchi

Japan Science and Technology Corporation–Precursory Research for Embryonic Science and Technology Project, Research Institute for Electronic Science, Hokkaido University, Kita-12 Nishi-6, Kita-ku, Sapporo 060-0812, Japan

Received November 14, 2000

Beamlike twin-photon generation by use of type II spontaneous parametric downconversion is demonstrated. The intensity distribution of each beam is round, and the emission angle is very small (0.9°). As a result, a high coincidence-count rate per unit of pump power was recorded. The ratio of coincidence-count rate to single-count rate was estimated to be 80% in this experiment. These features suggest that this method is useful for generation of a single-photon state and is applicable to bright, entangled twin-photon sources.

OCIS codes: 270.0270, 270.5290, 270.4180.

The creation of twin photons by use of spontaneous parametric downconversion has been a very important tool in exploring the nonlocal feature of quantum mechanics,[1] and recently in experiments in quantum information technology. Demonstrations of quantum teleportation with photons[2,3] are examples of these experiments. In the field of quantum cryptography,[4–7] spontaneous parametric downconversion should be an indispensable technique for generation of single-photon pulses,[8] quantum repeaters,[9] and so on. One of the reasons for the small bit rates of these experiments was that the photon pairs were radiated to a widely spreading region by the sources that were used, and it was difficult to utilize all the photon pairs. In addition, the intensity distribution of the photons selected by an iris was not symmetrical, which caused difficulties in the experiments.

In this Letter a new method of generating parametric fluorescence in two small spots is reported. Because the generated twin photons were concentrated on the spots, a high single-count rate and a high coincidence-count rate per unit of pump power were observed. It was also observed that the ratio of the coincidence-count rate to the single-count rate was 80% when the loss at the filters and the quantum efficiency of the detectors were normalized out.

When a laser pump beam is incident upon a nonlinear crystal, pairs of photons that satisfy the type II phase-matching conditions

$$\omega_p = \omega_e + \omega_o, \qquad \mathbf{k}_p = \mathbf{k}_e + \mathbf{k}_o \tag{1}$$

are emitted. Here, ω denotes angular frequency, $\mathbf{k}$ is the wave-number vector, and subscripts p, o, and e indicate the incident UV laser light and the fluorescence photons with ordinary and extraordinary polarization, respectively. Schemes of so-called tuning curves, which are plots of the signal (extraordinary-ray) and idler (ordinary-ray) wavelengths as a function of the crystal output angles, are shown in Fig. 1. When the angle ψ between the crystal angle and the pump-beam direction is given, the tuning curves can be calculated.[10] All tuning curves shown in Fig. 1 are for the planar case, in which the optic axis, $\mathbf{k}_p$, $\mathbf{k}_o$, and $\mathbf{k}_p$ all lie in the same plane. The wavelength of the pump beam is assumed to be 351.1 nm.

Figure 1(a) shows the case of the collinear condition, in which the signal and idler photons travel collinearly with the degenerate wavelength of 702.2 nm. The inset shows an image of the emitted twin photons at 702.2 nm as observed when one is facing the crystal. These twin photons are emitted into two cones that touch in the pump-beam direction. This condition has been widely used in experiments; however, here the collinear photons were selected by use of irises, and only a small portion of the whole ensemble of emitted photons was utilized. For example, a single-count rate of 3.4×10^3 cps and a coincident-count rate of 20 cps were reported with a 0.56-mm-thick β-BaB_2O_4 (BBO) type II crystal followed by spectral filters with 83-nm FWHM bandwidth and a collection lens with a 24.5-mm aperture.[11]

When the angle ψ is increased, the idler- and signal-beam curves overlap, as shown in Fig. 1(b). When the

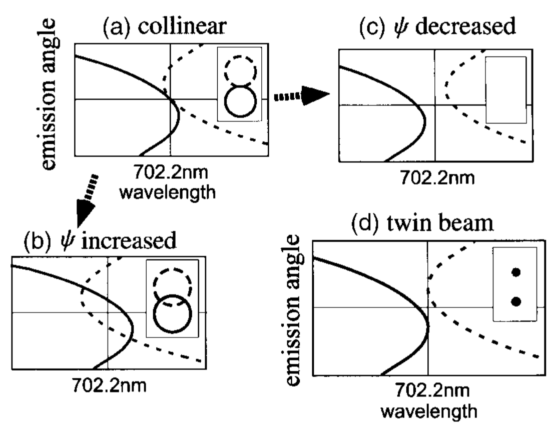

Fig. 1. Schematic of the tuning curves given in Ref. 8. The dashed curve indicates the idler beam, and the solid curve indicates the signal beam. The insets are images of the parametric fluorescence: (a) collinear condition, (b) angle ψ between the pump-beam direction and the crystal axis is increased, (c) ψ is decreased, (d) condition for twin-beam generation.

0146-9592/01/110843-03$15.00/0

photon pairs emitted into the overlapping sections are selected, the pairs are in an entangled state.[12] When ψ is decreased, these two curves move away from each other, and no photons are emitted at 702.2 nm [Fig. 1(c)].

The scheme for generating beamlike twin photons is shown in Fig. 1(d). When ψ is set such that the two curves are tangent to the line at the wavelength of 702.2 nm, twin photons will be emitted into two small regions. A schematic of the experimental setup is shown in Fig. 2. A 2-mm-diameter pump beam (150 mW) at wavelength 351.1 nm from a single-frequency-operated argon-ion laser is injected into a BBO crystal with a length of 5 mm. The BBO crystal is cut for a type II phase-matching situation ($\psi_0 = 48.9°$), such that the face of the crystal is almost normal to the pump beam for the collinear condition. The angle ψ between the pump-beam direction and the crystal axis is changed by use of a tilting stage. In the following, we use the parameter $\Delta\psi$ for the tilting angle from the condition in which the face is normal to the pump beam. For example, when $\Delta\psi = -1°$, one can calculate ψ as 47.9°. The parametric twins are imaged by a Peltier-cooled CCD camera with a focusing lens and a narrow-bandpass filter [center wavelength, 702.2 nm; FWHM, 0.32 nm (Ref. 13)].

When $\Delta\psi$ was decreased from the collinear condition, a ring-shaped image of parametric fluorescence was observed. As $\Delta\psi$ was decreased, the ring gradually shrank, and finally the image became a single filled circle at $\Delta\psi = -1.83°$. When $\Delta\psi$ was decreased further, the radius of the circle did not change much, and the intensity decreased. When $\Delta\psi$ became $-1.95°$, the parametric fluorescence vanished. A CCD image of the parametric beam and an intensity distribution with $\psi = -1.87°$ are shown in Fig. 3. The intensity distribution shows that the beam is symmetrical. In this case, the dispersion angle was 0.9°.

Next, the distribution of parametric fluorescence and the correlation between two parametric twin beams by the photon-counting method were measured. The photons were counted with single-photon-counting modules (SPCM-AQ221, EG&G) and a gated photon counter (SR400, Stanford Research Systems).

First, the distribution of parametric fluorescence was obtained for several values of $\Delta\psi$ by measurement of the single-count rate of detector A after the position of iris A, which was set 62 cm from the crystal. The diameter of iris A was 3 mm. The experimental results are shown in Fig. 4. The scan range of the iris position was ± 5 mm, which corresponds to the angle 0.93°. When $\Delta\psi$ was $-1.75°$, parametric fluorescence was emitted into the spreading cone (large ring), and therefore no peak was observed and the intensity was still small. The count rate at the center increased when $\Delta\psi = -1.79°$. Note that, since this scan was made across a ring, the counts would fall again on either side if the scan range were wider. Finally, the intensity distribution became almost flat in the scan area $\Delta\psi = -1.83°$, and the highest intensity was observed. A single-count rate of 4.1×10^5 cps was observed when the iris was removed. Considering the loss of optics and the quantum efficiency of detectors, we find that the compensated rate is $\sim 2 \times 10^6$ cps. As $\Delta\psi$ decreased, the intensity became lower and almost vanished when $\Delta\psi = -1.95°$.

The coincidence-count rate for $\Delta\psi = -1.83°$ was also measured. No iris was put into mode B, and the same iris A as that for the single-count measurement was used for scanning. The measured coincidence-count

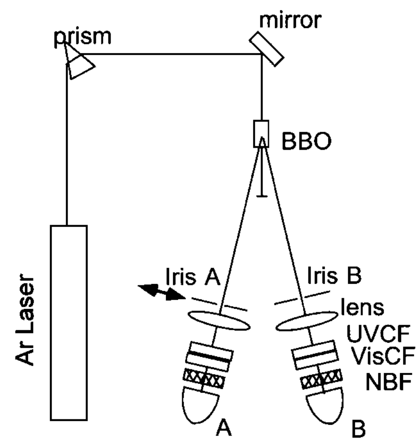

Fig. 2. Schematic of the experimental setup: UVCF, ultraviolet-light-cutting filter; VisCF, visible-light-cutting filter; NBF, narrow-band filter.

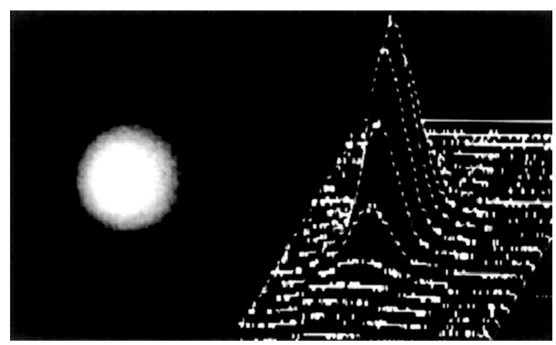

Fig. 3. Image of parametric fluorescence observed with a Peltier-cooled CCD camera. The intensity distribution of the image is shown on the right-hand side.

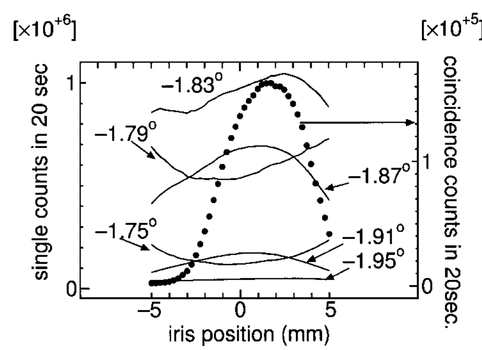

Fig. 4. Solid curves, single-count rates of photon detector A; $\Delta\psi$, tilting angle of the BBO crystal defined in the text; filled circles, coincidence counts of photon detectors A and B when the position of iris A at $\Delta\psi = -1.83°$ is changed. These data were obtained when the iris position in mode A was changed. Note that no iris was inserted in mode B. See the text for a detailed explanation.

rate is shown by the filled circles in Fig. 4. A coincidence-count rate of 8000 cps was observed at maximum. The highest coincidence count reported so far is believed to be 800 s^{-1} (Ref. 14) for 1-mW pump power with 5-nm bandwidth filters with two 0.6-mm-thick BBO crystals, where the filter transmissions and detector efficiencies were divided out. When we assume very simple linear scaling of the bandwidth, the estimated coincidence-count rate for the same situation as that reported in Ref. 14 is 4800 cps for the source used here.

In the present results, the ratio of the coincidence-count rate to the single-count rate was 15.2% at maximum. This ratio is affected by the transparency of the filters and the quantum efficiency of the detector. Because the bandwidth of the filters is much larger than the linewidth of the pump beam (7.5 MHz) and also is smaller than the spectrum of the parametric fluorescence,[15] the compensated ratio, α, is estimated as follows:

$$\alpha = \frac{N_{\mathrm{cc}} \eta_a \int t_{\mathrm{A}}(l) \mathrm{d}\lambda}{N_{\mathrm{A}} \eta_{\mathrm{A}} \eta_{\mathrm{B}} \int t_{\mathrm{A}}(\lambda) t_{\mathrm{B}}(\lambda_0 - \lambda) \mathrm{d}\lambda}, \qquad (2)$$

where N_{cc} is the coincidence count rate, N_{A} is the single-count rate, $\eta_{\mathrm{A(B)}}$ is the quantum efficiency of detector A(B), and $t_{\mathrm{A(B)}}\lambda$ is the transmittance of the filter in mode A(B) at wavelength λ. λ_0 denotes the degenerate wavelength (702.2 nm of the pump beam at 351.1 nm). In the experiment, $\eta_{\mathrm{A}} = \eta_{\mathrm{B}} = 0.7$. Since the measured functions $t_{\mathrm{A}}(\lambda)$ and $t_{\mathrm{B}}(\lambda)$ were well approximated by the same Gaussian function with center wavelength λ_0, it was estimated that α was 0.8. This result means that when we observe an idler photon we can find a single photon with a probability of 80%.

It was also found that the FWHM of the position dependence of the coincidence-count rate is equal to the aperture size of iris B, which was put at the same distance from the crystal as iris A. In the case shown in Fig. 4, no iris was inserted into mode B, but the aperture of the optics determined the width of the graph.

After submission of this Letter, I was informed that Monken *et al*. reported a high collection efficiency of 84%, obtained with a focusing lens in the pump beam for type II downconversion.[16] By adopting their technique, it may be possible to collimate the twin beams reported here into smaller spots.

In summary, beamlike twin-photon generation by use of type II spontaneous parametric downconversion has been demonstrated. The emitted angle was small (0.9°), and a symmetrical intensity distribution was obtained. The estimated ratio of the coincidence-count rate to the single-count rate was 0.8. These features all show that this method is useful for single-photon pulse generation by the gating method with high-quantum-efficiency multiphoton detectors[17,18] and may also be applicable to quantum information processing by use of photons.[19,20]

The author thanks T. Isu, S. Nishikawa, K. Tsujino, and K. Sasaki for fruitful discussions and T. Ogama for his support. This work was partly supported by the Japan Science and Technology—Core Research for Evolution Science and Technology project, Japan Society for the Promotion of Science grant 12555008, and Mitsubishi Electric Corporation. E-mail address, takeuchi@es.hokudai.ac.jp.

References

1. A. Einstein, B. Podolsky, and N. Rosen, Phys. Rev. **47,** 777 (1935).
2. D. Bouwmeester, J. W. Pan, K. Mattle, M. Eibl, H. Weinfurter, and A. Zeilinger, Nature (London) **390,** 575 (1997).
3. D. Boschi, S. Branca, F. De Martini, L. Hardy, and S. Popescu, Phys. Rev. Lett. **81,** 5039 (1998).
4. H. Zbinden, H. Bechmann-Pasquinucci, N. Gisin, and G. Ribordy, Appl. Phys. B **67,** 743 (1998).
5. T. Jennewein, C. Simon, G. Weihs, H. Weinfurter, and A. Zeilinger, Phys. Rev. Lett. **84,** 4729 (2000).
6. D. S. Naik, C. G. Peterson, A. G. White, A. J. Berglund, and P. G. Kwiat, Phys. Rev. Lett. **84,** 4733 (2000).
7. W. Tittel, J. Brendel, H. Zbinden, and N. Gisin, Phys. Rev. Lett. **84,** 4737 (2000).
8. C. K. Hong, Z. Y. Ou, and L. Mandel, Phys. Rev. A **59,** 2044 (1987).
9. H. J. Briegel, W. Dür, J. I. Cirac, and P. Zoller, http://xxx.lanl.gov.abs/quantu-ph/9803056.
10. T. B. Pittman, D. V. Strekalov, D. N. Klyshko, M. H. Rubin, A. V. Sergienko, and Y. H. Shih, Phys. Rev. A **53,** 2804 (1996).
11. A. V. Sergienko, Y. H. Shih, and M. H. Rubin, J. Opt. Soc. Am. B **12,** 859 (1995).
12. P. G. Kwiat, K. Mattle, H. Weinfurter, A. Zeilinger, A. V. Sergienko, and Y. Shih, Phys. Rev. Lett. **75,** 4337 (1995).
13. These narrow bandwidths will be used for future interference experiments.
14. P. G. Kwiat, E. Waks, A. G. White, I. Appelbaum, and P. H. Eberhard, Phys. Rev. A **60,** R773 (1999).
15. **It** is because the size of the spot did not change when another filter of 1.0-nm FWHM was used.
16. C. H. Monken, P. H. S. Ribeiro, and S. Pauda, Phys. Rev. A **57,** R2267 (1998).
17. S. Takeuchi, J. Kim, Y. Yamamoto, and H. H. Hogue, Appl. Phys. Lett. **74,** 1063 (1999).
18. J. Kim, S. Takeuchi, Y. Yamamoto, and H. H. Hogue, Appl. Phys. Lett. **74,** 902 (1999).
19. S. Takeuchi, Phys. Rev. A **62,** 032301 (2000).
20. S. Takeuchi, Phys. Rev. A **61,** 052302 (2000).